Exact hydrodynamic solution for the elliptic flow

Robi Peschanski[1,*] and Emmanuel N. Saridakis[2,†]

[1]*Institut de Physique Théorique, CEA, IPhT, and Centre National de la Recherche Scientifique (CNRS), URA 2306, F-91191 Gif-sur-Yvette, France*

[2]*Department of Physics, University of Athens, GR-15771 Athens, Greece*

(Received 15 June 2009; revised manuscript received 7 August 2009; published 28 August 2009)

Looking for the underlying hydrodynamic mechanisms determining the elliptic flow we show that for an expanding relativistic perfect fluid the transverse flow may derive from a solvable hydrodynamic potential, if the entropy is transversally conserved and the corresponding expansion is "quasi-stationary," that is, mainly governed by the temperature cooling. Exact solutions for the velocity flow coefficients v_2 and the temperature dependence of the spatial and momentum anisotropy are obtained and shown to be in agreement with the elliptic flow features of heavy-ion collisions.

DOI: 10.1103/PhysRevC.80.024907 PACS number(s): 24.10.Nz, 12.38.Mh

I. INTRODUCTION

The hydrodynamic description of the formation and development of a quark-gluon plasma (QGP) in high-energy heavy-ion collisions has met with considerable success [1]. In particular, the hydrodynamic features seem to be, at least partly, required to take into account the second Fourier coefficient v_2 of the transverse flow of particles, the so-called *elliptic flow*. One writes [2,3] for the azimuthal multiplicity distribution

$$\frac{dN}{d\varphi} = \frac{N}{2\pi}\{1 + 2v_2\cos(2\varphi) + \cdots\}, \tag{1}$$

discarding for simplicity other Fourier coefficients that are nonrelevant here. The experimentally observed values of v_2, which are due to the anisotropy of the initial state collisions at nonzero impact parameter, are sizable enough to require important collective effects of particle production. These are better reproduced by hydrodynamical properties of the flow in some early stage of the quark-gluon plasma formation.

The theoretical estimates of the elliptic flow are obtained from numerical studies based on various versions of the hydrodynamic models. Indeed, a full study requires that one not only deal with the solution of the relativistic hydrodynamic equations but also with the definition of appropriate initial conditions and a model for the mutation of the QGP pieces of fluid into particles. The numerical studies (cf. Ref. [1]) reveal that the QGP as a fluid is "almost perfect" because its viscosity is remarkably weak, even if the model dependence may account for some variation on the quantitative estimates. This observation has a considerable theoretical impact, because it points to a strongly coupled plasma, guiding a large part of theoretical interest toward strongly coupled gauge field theories.

Our goal in the present work is to try and identify by explicit analytic solutions the basic hydrodynamic mechanisms at work in the elliptic flow. For this, we must simplify (or even idealize) the description of the QGP formation in a heavy-ion collision while keeping the main physical ingredients. Among other simplifications that we discuss now, our study assumes the QGP to be a perfect fluid without viscosity. We also restrict our analysis to the transverse flow in the central rapidity region where the hydrodynamic description is better suited.

The main characteristic feature of the hydrodynamic description of QGP formation in heavy-ion collisions appears to be a nontrivial combination of: (a) the large longitudinal momentum and energy boosts provided to the created medium by the initial state, and (b) the (presumably fast) equilibration of the energy density and all three pressure components due to local thermalization required by hydrodynamics. As a matter of fact, the first stage of the hydrodynamical description of particle production in high energy collisions is mainly governed by the longitudinal flow, that is, the expansion of the relativistic fluid in $(1 + 1)$ dimensions. The authors of the pioneering articles of the hydrodynamic approach [4,5] based their analysis on this property.

In the mean time, the four-dimensional hydrodynamical feature of the system is kept with the thermodynamic relations which, through the local temperature T and the equation of state (EoS), lead to

$$\frac{T}{T_0} \sim \left(\frac{\tau_0}{\tau}\right)^{c_s^2}; \quad \tau \equiv \sqrt{x_0^2 + x_3^2}; \quad c_s^2 = \frac{dp}{de} = \frac{sdT}{Tds}, \tag{2}$$

where τ is the proper time; c_s is the speed of sound, which we assume to be constant in the following; and e and p are the energy and (isotropic) pressure density, respectively. Our remaining notations are s for the entropy density, $x_{\mu=\{0,\cdots 3\}}$ for the space-time coordinates ($x_0 \equiv t$), and $u_{\mu=\{0,\cdots 3\}}$ for the fluid four-velocity (with lower indices) in the Minkowski metric $\eta^{\mu\nu}$, with signature $(1, -1, -1, -1)$ satisfying the normalization condition

$$u_\mu u^\mu \equiv u_0^2 - u_3^2 - u_\perp^2 = 1; \quad u_\perp^2 \equiv u_1^2 + u_2^2. \tag{3}$$

Our idea for studying the transverse motion of the fluid is that it is also driven by the longitudinal evolution, but slowly enough to be considered "quasi-stationary," that is, in such a way that its time evolution is essentially related to the temperature cooling. Indeed, the seed of transverse momenta

*robi.peschanski@cea.fr
†msaridak@phys.uoa.gr

is indirect and there should be, at least during some first stage of the hydrodynamic evolution, no strong back-reaction on the longitudinal motion. The quasi-stationarity hypothesis allows for an exact solution for the elliptic flow and in general for the hydrodynamic regime in the transverse plane. To be concrete we state the following conjectured properties of the hydrodynamic flow:

(i) *Tranversally isentropic.* Because the overall entropy should be conserved, we conjecture that the transverse flow is itself (approximately) isentropic; i.e., we write the following equation

$$[\partial_{x_1}(su_1) + \partial_{x_2}(su_2)]_{\text{transverse}} = 0. \tag{4}$$

(ii) *Quasi-stationary.* Because the time dependence of the transverse entropy distribution is absent from Eq. (4), we close the equations for the transverse flow by assuming that its hydrodynamic evolution is smooth enough to be driven only by the temperature change. We thus consider the equation and solutions of a temperature-dependent stationary flow, with a source emitting a fluid at a given temperature (and thus transverse speed, see further).

Hence, in the regime when the longitudinal expansion is dominant, the transverse motion is conjectured to be smoothly driven by the overall local temperature of the fluid, which provides the four-dimensional feature[1] of the system through the thermodynamic relations (2).

The plan of the article is the following: In Sec. II, using the hydrodynamic potential for a stationary flow [7], we derive the analytic equation obeyed by the azimuthal distribution of entropy and thus the elliptic flow. Then, in Sec. III, we find the exact solutions for the transverse flow. In Sec. IV we apply our solution showing that the obtained elliptic flow retains good qualitative features observed in reality or in realistic numerical hydrodynamic model studies. A discussion of the hypotheses and our conclusions and outlook form the final section, Sec. V.

II. AZIMUTHAL ENTROPY DISTRIBUTION

As we see now, the conditions (a) and (b) lead to nontrivial properties of the fluid and to analytic solutions for the elliptic flow. Elliptic flow is obtained from a hydrodynamic (KK) potential [7] derived by Khalatnikov and Kamenshchik for a stationary transverse isentropic flow. The quasi-stationary hypothesis allows us to extend its applicability to a slow transverse motion of the fluid and to find the general exact solution of the elliptic flow. In fact, the existence of a hydrodynamical potential obeying a linear equation has long been known [8,9] for the longitudinal evolution. Recently [10], it was possible to express interesting analytic solutions for the entropy distribution dS/dy, where the (hydrodynamic) rapidity is defined by $y = \frac{1}{2}\log(u_0+u_3)/\log(u_0-u_3)$. We follow the same method as in Ref. [10] for the transverse flow case and find the general solution of the KK potential to obtain the azimuthal distribution of the entropy $dS/d\varphi$ giving access to the elliptic flow.

However, one crucial difference of the transverse with respect to the longitudinal case is the velocity-temperature relation between u_0, the time component of the velocity (and thus also $u_\perp = \sqrt{u_0^2-1}$, the modulus of the transverse one), and the local temperature. This comes from the relativistic Bernoulli relation, verified by a stationary fluid [11], namely

$$Tu_0 = T\sqrt{1+u_\perp^2} = T_0. \tag{5}$$

Under the same conditions, the whole evolution from some initial temperature to the final freeze-out, one is constrained to be in the *supersonic* regime [11], as we verify later through our equations. The condition is written as

$$v_\perp \equiv \frac{u_\perp}{u_0} = \frac{u_\perp}{\sqrt{1+u_\perp^2}} = \left\{1-\left(\frac{T}{T_0}\right)^2\right\}^{1/2} \geqslant c_s. \tag{6}$$

Hence, the isentropic transverse evolution starts at a given temperature T_I such that

$$T_I \leqslant T_s \equiv T_0\sqrt{1-c_s^2}, \tag{7}$$

and the velocity increases when the temperature decreases from T_I, reaching eventually ultrarelativistic values before hadronization. For convenience, we now introduce the variable

$$l = \frac{1}{2}\log\left[1-\left(\frac{T}{T_0}\right)^2\right] = \frac{1}{2}\log\left[\frac{u_\perp^2}{1+u_\perp^2}\right] = \log v_\perp. \tag{8}$$

The derivation of the KK potential is described briefly as follows [7]: Together with the transverse entropy conservation (4), the equations for the transverse flow close with the projection to the transverse plane of the energy-momentum conservation relation $\partial_\mu T_{nu^\mu} = 0$, again by neglecting the time derivatives with respect to the transverse gradients. After nontrivial transformations, presented in the Appendix, one obtains the following system of equations:

$$\begin{aligned} \partial_{x_1}(su_1) + \partial_{x_2}(su_2) &= 0 \\ \partial_{x_1}(Tu_2) - \partial_{x_2}(Tu_1) &= 0. \end{aligned} \tag{9}$$

Then, using the "hodograph" [7–11] inversion of variables $(x_1,x_2) \to (l,\varphi)$ and combining Eqs. (4) and (9), one arrives at the formulas expressing the kinematic (now dynamical) variables (x_1,x_2) in terms of the hydrodynamic variables through a suitably defined KK potential function $\chi(\varphi,l)$,

[1] In that respect, our picture is different from a purely transverse hydrodynamic flow [6].

namely

$$x_\perp(\varphi,l)=\frac{e^{-l}}{T_0}\sqrt{\left(\frac{\partial\chi}{\partial l}\right)^2+\left(\frac{\partial\chi}{\partial\varphi}\right)^2}$$
$$\alpha(\varphi,l)=\varphi+\arctan\left[\frac{\partial\chi}{\partial\varphi}\left(\frac{\partial\chi}{\partial l}\right)^{-1}\right], \tag{10}$$

where we have parametrized

$$u_1=u_\perp\cos\varphi \quad u_2=u_\perp\sin\varphi$$
$$x_1=x_\perp\cos\alpha \quad x_2=x_\perp\sin\alpha. \tag{11}$$

The KK potential function $\chi(\varphi,ul)$ is the solution of a linear equation obtained by closing the hydrodynamic equations system using the EoS

$$\left(1-\frac{e^{2l}}{c_s^2}\right)\frac{\partial^2\chi}{\partial\varphi^2}+(1-e^{2l})\frac{\partial^2\chi}{\partial l^2}+\left(1-\frac{1}{c_s^2}\right)e^{2l}\frac{\partial\chi}{\partial l}=0. \tag{12}$$

Note the zero coefficient at $e^l=c_s$, which signals the supersonic bound (6), (7) at $T=T_s$. In fact the system expands in the vacuum for $T\leqslant T_s$, whereas it is compressed when $T>T_s$ (cf. Ref. [4]). Hence the physical solutions are restricted to the supersonic range $T\leqslant T_I\leqslant T_s$.

The KK potential and its equation have been reproduced from Ref. [7]. The calculation of the entropy distribution is now parallel to the one [10] (see Ref. [12] for an early version) used in the $(1+1)$ dimensional case. Considering an entropy flux normal to the tangential line element (dx_1,dx_2), one must compute

$$dS=su_2dx_1-su_1dx_2. \tag{13}$$

Using the formulas [Eq. (10)] for the expression of the line element in terms of the potential, one has

$$-\frac{e^{-l}}{T_0}\frac{\partial\chi}{\partial l}=x_1\cos\varphi+x_2\sin\varphi=x_\perp\cos(\alpha-\varphi)$$
$$-\frac{e^{-l}}{T_0}\frac{\partial\chi}{\partial\varphi}=x_2\cos\varphi-x_1\sin\varphi=x_\perp\sin(\alpha-\varphi), \tag{14}$$

which, by differentiation with respect to l and ϕ, gives

$$dS=\frac{sT_0}{T}\left\{\left[\frac{\partial^2\chi}{\partial l\partial\varphi}-\frac{\partial\chi}{\partial\varphi}\right]dl+\left[\frac{\partial^2\chi}{\partial\varphi^2}+\frac{\partial\chi}{\partial l}\right]d\varphi\right\}, \tag{15}$$

where we used the relation $u_\perp e^{-l}\equiv u_0=T_0/T$.

At fixed temperature (and thus fixed l), which is the case considered further on, one gets the azimuthal entropy distribution

$$\frac{dS}{d\varphi}=\frac{sT_0}{T}\left[\frac{\partial^2\chi(\varphi,l)}{\partial\varphi^2}+\frac{\partial\chi(\varphi,l)}{\partial l}\right]$$
$$=\frac{sT}{T_0\left(1-e^{2l}/c_s^2\right)}\left[\frac{\partial\chi(\varphi,l)}{\partial l}-\frac{\partial^2\chi(\varphi,l)}{\partial l^2}\right], \tag{16}$$

where the second expression comes from the KK potential equation (12). Note again the singular coefficient at T_s, corresponding to the lower bound of temperature.

III. EXACT SOLUTION OF THE TRANSVERSE FLOW

In our idealized hydrodynamic framework, without hadronization, one relates the entropy distribution to multiplicity, $dS/S\sim dN/N$. Hence, the elliptic flow is defined by the azimuthal entropy distribution (16) through a Fourier expansion similar to Eq. (1), namely

$$\frac{dS}{d\varphi}=\frac{S}{2\pi}\{1+2v_2\cos(2\varphi)+\cdots\}, \tag{17}$$

and thus

$$v_2=\frac{\int d\varphi\,\cos(2\varphi)\,\frac{dS}{d\varphi}(\varphi)}{\int d\varphi\,\frac{dS}{d\varphi}(\varphi)}. \tag{18}$$

The eccentricity can be obtained as a function of temperature (or l) through Eq. (14) in terms of the KK potential $\chi(\varphi,l)$ as

$$\varepsilon\equiv\frac{\langle x_2^2-x_1^2\rangle}{\langle x_2^2+x_1^2\rangle}\equiv\frac{\int d\varphi\big(x_2^2(\varphi,l)-x_1^2(\varphi,l)\big)}{\int d\varphi\big(x_2^2(\varphi,l)+x_1^2(\varphi,l)\big)}$$
$$=\frac{\int d\varphi\left\{\cos2\varphi\left[\left(\frac{\partial\chi}{\partial\varphi}\right)^2-\left(\frac{\partial\chi}{\partial l}\right)^2\right]+2\sin2\varphi\,\frac{\partial\chi}{\partial\varphi}\,\frac{\partial\chi}{\partial l}\right\}}{\int d\varphi\left[\left(\frac{\partial\chi}{\partial\varphi}\right)^2+\left(\frac{\partial\chi}{\partial l}\right)^2\right]}. \tag{19}$$

Note the characteristic feature of the hodograph method: a geometrical parameter, here ε, is expressed in terms of dynamical ones, here the temperature. Once the solution is found, one must invert these relations to restore the hierarchy between "cause" and "effect."

We can now proceed by looking for the general solution resulting from the KK potential solution of Eq. (12). For this, it is convenient to expand the potential

$$\chi(\varphi,l)=\beta_0(l)+\sum_{p=1}^{\infty}\beta_p(l)\cos(2p\,\varphi) \tag{20}$$

in Fourier coefficients $\beta_p(l)$ that verify the equation

$$(e^{2l}-1)\beta_p''(l)+e^{2l}\big(c_s^{-2}-1\big)\beta_p'(l)$$
$$-4p^2\big(c_s^{-2}e^{2l}-1\big)\beta_p(l)=0, \tag{21}$$

where primes denote derivatives with respect to l.

As is well known, the solution is in general a suitable combination, with constant coefficients, of two independent solutions of the second-order equation (20). Using standard textbooks, one finds for $p\neq0$

$$\begin{aligned}\beta_p(l) &= c_p^{(1)}\beta_p^{(1)} + c_p^{(2)}\,\beta_p^{(2)} \\ &\equiv c_p^{(1)}\,(-)^{p+1}e^{2pl}\,{}_2F_1\left(p+\frac{1}{4}\left\{c_s^{-2}-1\right\}-\sqrt{\left\{c_s^{-2}-1\right\}^2/16+c_s^{-2}p^2},\, p+\frac{1}{4}\left\{c_s^{-2}-1\right\}\right. \\ &\quad \left.+\sqrt{\left\{c_s^{-2}-1\right\}^2/16+c_s^{-2}p^2},\, 1+2p;\, e^{2l}\right) \\ &\quad + c_p^{(2)}G^{2,0}_{2,2}\left(e^{2l}\left|\begin{matrix}\frac{5-c_s^{-2}}{4}-\sqrt{\left(\frac{c_s^{-2}-1}{4}\right)^2+c_s^{-2}p^2} & \frac{5-c_s^{-2}}{4}+\sqrt{\left(\frac{c_s^{-2}-1}{4}\right)^2+c_s^{-2}p^2} \\ -p & p\end{matrix}\right.\right),\end{aligned} \tag{22}$$

while we single out the first component $c_0\,\beta_0(l)$, whose derivative is simply written as

$$\beta_0'(l) = (1-e^{2l})^{\frac{1-1/c_s^2}{2}}. \tag{23}$$

In Eq. (22), ${}_2F_1(a,b;c,z)$ is the usual hypergeometric function, while $G^{2,0}_{2,2}\left(e^{2l}\left|\begin{matrix}a & b\\ c & d\end{matrix}\right.\right)$ denotes a Meijer function [13].

The function $\beta_p^{(1)}$ (resp. $\beta_p^{(2)}$) is the regular (resp. irregular) solution[2] at $e^l = 0$ of Eq. (21). Hence, any arbitrary combination of these two independent functions is a solution of Eq. (21). The boundary conditions define the specific linear combinations to be chosen for the general solution that may be obtained from the Green function of the problem. For illustration, in the special case $p = 0$, one writes

$$\beta_0'(l) = \int_{-\infty}^{+\infty}\Theta(-l)\left(1-e^{2(l-\hat{l})}\right)^{\frac{1-c_s^{-2}}{2}}F_0(\hat{l})d\hat{l}, \tag{24}$$

where $F_0(l)$ describes a distribution of sources in temperature convoluted with the Green function, which in this case is just $\Theta(-l)\,\beta_0'(l)$ from Eq. (23). A straightforward but more tedious expression can be written for all values of p but is skipped here for brevity. A specific realization for the sake of our physical problem is discussed in the applications section (Sec. IV).

Inserting the general solution [Eqs. (20) and (22)] for the KK potential in Eq. (16) for the azimuthal entropy distribution, one finds

$$\frac{dS}{d\varphi}(\varphi) = \frac{sT_0}{T}\left\{\beta_0'(l)+\sum_{p=1}^{\infty}\cos(2p\varphi)\left[(2p)^2\beta_p(l)-\beta_p'(l)\right]\right\}$$

$$\begin{aligned}v_2(T) &= \frac{4\beta_1(l)-\beta_1'(l)}{2\beta_0'(l)} \\ &\equiv \rho\left[\frac{4\beta_1^{(1)}(l)-\beta_1'^{(1)}(l)}{2\beta_0'(l)}+\lambda\,\frac{4\beta_1^{(2)}(l)-\beta_1'^{(2)}(l)}{2\beta_0'(l)}\right],\end{aligned} \tag{25}$$

where we denote $\frac{c_1^{(1)}}{c_0}\equiv\rho$, $\frac{c_1^{(2)}}{c_1^{(1)}}\equiv\lambda$, and

$$\varepsilon(T) = \frac{2\beta_0'(l)[2\beta_1(l)+\beta_1'(l)]+\sum_{p=1}^{\infty}[4p(p+1)\beta_p(l)\beta_{(p+1)}(l)+2p\beta_p(l)\beta_{p+1}'(l)-2(p+1)\beta_{p+1}(l)\beta_p'(l)-\beta_p'(l)\beta_{p+1}'(l)]}{2\beta_0'^2(l)+\sum_{p=1}^{\infty}[(2p\beta_p(l))^2+\beta_p'^2(l)]} \tag{26}$$

for the eccentricity. It is useful for further use to note that, in the "elliptic approximation," i.e., when one stops the Fourier expansion (20) at $p = 1$, the eccentricity can be expressed using the same functions and parameters with v_2 as in Eq. (25), namely

$$\begin{aligned}\varepsilon(T) &= \frac{2\beta_0'(l)[2\beta_1(l)+\beta_1'(l)]}{2\beta_0'^2(l)+\left[4\beta_1^2(l)+\beta_1'^2(l)\right]} \\ &\equiv \rho\left\{\frac{2\beta_0'\left[2\left(\beta_1^{(1)}+\lambda\beta_1^{(2)}\right)+\beta_1^{(1)'}+\lambda\beta_1^{(2)'}\right]}{2\beta_0'^2+\rho^2\left[4\left(\beta_1^{(1)}+\lambda\beta_1^{(2)}\right)^2+\left(\beta_1^{(1)'}+\lambda\beta_1^{(2)'}\right)^2\right]}\right\}.\end{aligned} \tag{27}$$

Thanks to the analytic solutions we obtained, all the expressions contain an explicit dependence on temperature. One

[2]For $p = 0$, Eq. (21) is only first-order for $\beta_0'(l)$ and thus introduces only one arbitrary coefficient c_0.

should only specify which temperature is physically relevant, e.g., T_I for the initial spatial eccentricity and some freeze-out temperature T_f for the observed v_2. Using our formulas, one may discuss the dynamical hydrodynamical process through the temperature dependence of both the spatial and the momentum average anisotropy of the lump of quark-gluon plasma. For this, we note an interesting parameter-independent relation between the spatial eccentricity at any temperature T_I and v_2 at any temperature T_f, namely

$$\frac{v_2(T_f)}{\varepsilon(T_I)} = \frac{\beta_1(T_f)\beta'(T_I)}{\beta_1(T_I)\beta'(T_f)} \times \frac{1-\frac{\beta_1'(T_f)}{2\beta_1(T_f)}}{1+\frac{\beta_1'(T_I)}{2\beta_1(T_I)}} \times \left(\frac{1}{2}+\frac{1}{2}\sqrt{1-2\varepsilon^2(T_I)\,\frac{1+\frac{\beta_1'^2(T_I)}{4\beta_1^2(T_I)}}{\left(1+\frac{\beta_1'(T_I)}{2\beta_1(T_I)}\right)^2}}\right)^{-1}. \quad (28)$$

A general physical comment is in order about the parameters λ and ρ defining the relevant solutions in the "elliptic approximation." Using a source of given temperature, the parameter λ, which corresponds to the relative strength of the two independent solutions of the second-order differential equation (21), will specify the initial condition of the elliptic flow. The parameter ρ, which is geometrical in nature because it gives the relative strength of the elliptic harmonic in Eq. (20), will be related to the initial centrality of the reaction. For general initial conditions, the more general Green function formalism, cf. Eq. (24), must be used.

IV. EXACT ELLIPTIC FLOW: APPLICATIONS

Taking into account the linear equations for the potential and entropy distributions, cf. Eqs. (12) and (15), the determination of the elliptic flow boils down to defining properly the boundary conditions, i.e., the sources of the hydrodynamic expansion, which are given functions of temperature and azimuth. In the following we assume that the source is simply given by a δ function at the initial temperature T_I of the process and a given initial eccentricity profile. We fix it by the condition that $v_2(T_I) = 0$ while $\varepsilon(T_I)$ is maximal. Note that the solution satisfies the constraint $T_I \lesssim T_s$, i.e., the fluid is always supersonic.

In the "elliptic approximation" for which the Fourier expansion of the potential (20) is limited to the two first orders, the observables v_2 (25) and ε (27) depend only on two relevant parameters, namely $\rho = c_1^{(1)}/c_0$, obtained from the Fourier expansion (20) and $\lambda = c_1^{(2)}/c_1^{(1)}$, that is, the coefficient ratio between the regular and irregular solutions (22) of the potential equations (12),(21).

Determination of λ. From the previous discussion, λ is chosen in such a way that $v_2(T_I) = 0$, where $\varepsilon(T_I)$ is maximal. As an illustration of the discussion, the temperature dependence of both v_2 and ε that we obtain with our definition of the initial condition is displayed in Fig. 1 for a given value of the geometrical anisotropy parameter $\rho = 0.8$. The value of T_I is lower but near the speed-of-sound lower limit of temperature T_s.

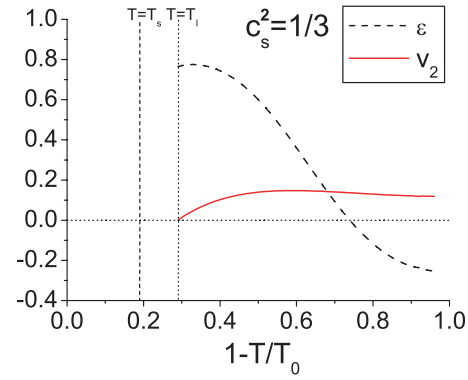

FIG. 1. (Color online) Compared temperature dependence for the momentum $v_2(T)$ and the spatial $\varepsilon(T)$ anisotropies. The curves correspond to the initial temperature source at $T = T_I$ (see text). The dashed line is for the supersonic lower bound T_s. The geometrical anisotropy parameter (see text) is $\rho = 0.8$ and the speed of sound is the reference one $c_s = 1/\sqrt{3}$.

Determination of ρ. The determination of the geometrical parameter ρ, the first anisotropy coefficient of the potential χ, see Eq. (20), is governed by the centrality. In Fig. 2 we display $\varepsilon(\rho)$, which shows a quasi-linear behavior. This is in good agreement with the observed feature of the experimentally reconstructed eccentricity with an observed proportionality relation with the centrality $c \sim N_{\rm part}/N_{\rm max}$, where $N_{\rm part}$ is the number of participant nucleons. Indeed, one expects a simple relation between ρ and c, up to a rescaling $\rho/\rho_{\rm max} \sim 1 - N_{\rm part}/N_{\rm max}$. With such a choice and using Eq. (25), one finds a simple proportionality rule of v_2 with centrality, namely

$$v_2 = \rho_{\rm max}(1-c) \times \left[\frac{4\beta_1^{(1)}(l) - \beta_1'^{(1)}(l)}{2\beta_0'(l)} + \lambda\frac{4\beta_1^{(2)}(l) - \beta_1'^{(2)}(l)}{2\beta_0'(l)}\right], \quad (29)$$

which is also expected from hydrodynamical simulations [14]. Note that, in this framework, $\rho_{\rm max}$ is indeed independent of the evolving temperature ratio T/T_0, but it may depend on the initial conditions such as the type of heavy-ion reaction and the initial center of mass energy (or T_0). The T/T_0 dependence,

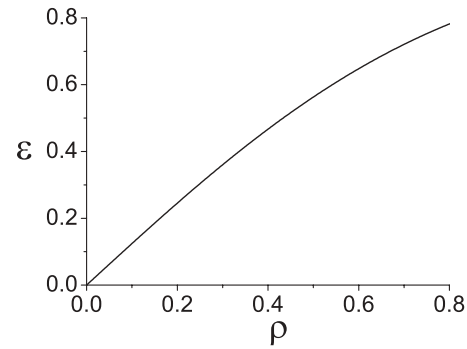

FIG. 2. ε as a function of the geometrical anisotropy parameter ρ. The observed dependence qualitatively reproduces simulations of ε as a function of centrality $c \sim N_{\rm part}/N_{\rm max}$ (see text). In this figure we use $c_s^2 = 1/3$ and $\rho_{\rm max} \sim 0.8$.

given in Eq. (29) by the function within brackets, is uniquely defined from (25). In our calculations, the linearity of Eq. (25) for v_2 in terms of the normalized second Fourier coefficient ρ is a direct consequence of the Eq. (12) for the KK potential, which, together with the azimuthal entropy distribution, is diagonalized by the Fourier expansion (20). It is clear that the formulation of the initial eccentricity profile depends on the initial conditions, and we take the curve in Fig. 2 as an example.

Figure 1 is interesting also from the point of view of the dynamics of elliptic flow. Indeed, it is known from hydrodynamic models [14] that the *momentum anisotropy*, represented in our quasi-stationary approximation by the temperature-dependent $v_2(T)$, rapidly increases as a function of proper time, and thus with decreasing temperature, to reach its observed value. It is therefore confirmed to be a good indicator of the early stage of the hydrodynamic expansion. On the same footing, the *spatial anisotropy*, represented by $\varepsilon(T)$, decreases as the system expands, even reaching negative values, i.e., changing the sign of the spatial anisotropy. We observe, in Fig. 1, that the transversally isentropic flow follows the same qualitative path as a function of temperature cooling. It is also interesting to note that the final value of v_2 (and thus the value of v_2/ε, where $\varepsilon \equiv \varepsilon(T_I)$ is the initial eccentricity) is reached rather early and rather independently of the choice of the initial temperature for the transverse flow.

To restore the time variable through its dependence on the temperature, we shall make use of a convenient rescaling of the temperature equivalent to the expansion time, similar to the one proposed in Ref. [15], where the ratio $v_2(\tau-\tau_0)/\varepsilon(\tau_0)$ with initial time τ_0 is displayed for different values of impact parameter and various values of the speed of sound c_s. One makes the rescaling substitution

$$\tau \to \frac{c_s}{\bar{R}}(\tau-\tau_0); \quad \frac{1}{\bar{R}} = \sqrt{\frac{1}{\langle x_1^2\rangle}+\frac{1}{\langle x_2^2\rangle}}. \tag{30}$$

where $\bar{R}$ gives an appropriate average estimate of the expanding size of the plasma. In our temperature-dependent scheme, we define an analogous rescaling using the thermodynamical relation (2) by choosing a "rescaled time" variable defined in terms of the temperature as

$$\theta \equiv \frac{c_s}{\bar{R}}\left\{\left(\frac{T_0}{T}\right)^{c_s^{-2}} - \left(\frac{T_0}{T_I}\right)^{c_s^{-2}}\right\}. \tag{31}$$

In Fig. 3 we show the theoretical results for v_2/ε as a function of the rescaled variable θ for the solution we considered. Let us comment on both parts of the figure. On the top, the figure displays the dependence on centrality via $\rho = \rho_{\max}(1-c)$. The value of $\rho_{\max}$ has been chosen fixing $v_2(\tau-\tau_0)/\varepsilon(\tau_0)$ to match with some realistic value (see, e.g., Refs. [1,14]). One observes the general trend of the θ evolution as a function of increasing centrality (or decreasing ρ). This trend, which has been empirically observed in hydrodynamic simulations [15] is here explained by the nonlinear ε-dependent correction to v_2/ε [see Eq. (28)]. It is easy to realize that the remnant ε dependence in Eq. (28) is such that it increases for increasing ε (the denominator is smaller) and thus it decreases with

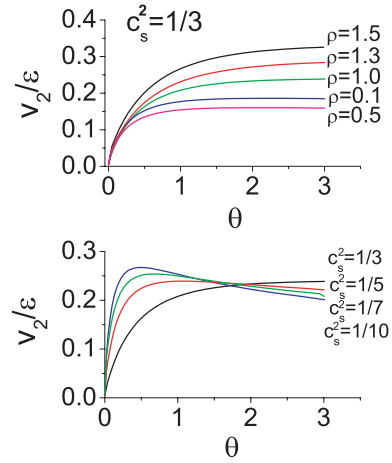

FIG. 3. (Color online) v_2/ε as a function of the "rescaled time" θ. (Top) Dependence on the centrality via the ρ parameter at fixed $c_s = 1/\sqrt{3}$. (Bottom) Dependence on the EoS via $c_s^2 = (1/3, 1/5, 1/7, 1/10)$ at fixed eccentricity $\varepsilon = 0.8$. For this, one is led to choose, respectively, $\rho = (0.8, 1, 2, 4)$, by tuning the values of $\rho_{\max}$. The "reduced time" is defined by Eq. (31).

centrality. Hence our scheme reproduces, at least qualitatively, a trend as a function of an impact parameter observed in hydrodynamical simulations.

Also, in the bottom graph of Fig. 3 we display the speed-of-sound dependence of $v_2(\theta)/\varepsilon$. Thanks to the "time" rescaling (30), it is possible to superimpose the different curves, provided an adequate choice of ρ ensures the constant initial $\varepsilon(T_I)$. As also seen numerically, the analytical dependence over c_s of our resulting formula (28) gives a decreasing value of the ratio $v_2(\theta)/\varepsilon(T_I)$ with decreasing speed of sound. Here also one finds the observed behavior [15]. However, this hierarchy is obtained at rather larger θ than observed in Ref. [15]. We comment on that feature in the next section.

V. CONCLUSION, DISCUSSION, AND OUTLOOK

Let us briefly summarize our results: using the conjecture of a quasi-stationary and transversally isentropic hydrodynamic regime governing the transverse flow, and for a given EoS, we arrive at a closed system of hydrodynamic equations that can be solved by the hodograph transform $x_{1,2} \to T, \varphi$. Thanks to the potential method [7] we can formulate the general solution and give explicit analytic expressions for the hydrodynamic features of the transverse flow. In an application to a source with given temperature and constant effective speed of sound c_s, we are able to give a complete analytic solution. The applications to the determination of the features of the elliptic flow are in good qualitative agreement with the observed (or numerical) characteristics: the temperature dependence of the spatial and velocity anisotropy (see Fig. 1), the linear behavior of v_2 with centrality [cf. Eq. (29)] for a realistic initial eccentricity (see Fig. 2), and the centrality and speed of sound dependence of the ratio v_2/ε (see Fig. 3).

Now, possessing an analytic solution, it is possible to go back to the initial assumptions and discuss their range of validity. In other terms we may address the question of

which approximation can we consider our closed system of transverse equations to be a good approximation of the full hydrodynamic equations. To quantify this approximation a meaningful comparison is to give estimates of two quantities that are relevant for the discussion of the two hypotheses: (a) a transversally isentropic flow and (b) a quasi-stationary transverse flow.

To test our conjecture (a) and looking to Eq. (4), we are led to consider the following ratio of entropy flow gradients:

$$\frac{\partial_{x_\perp}(su_\perp)}{\partial_\tau(su_0)} \sim \frac{\partial_T(su_\perp)}{\partial_T(su_0)} \Big/ \frac{\partial_T x_\perp(T)}{\partial_T \tau(T)} \equiv \frac{1}{\mathcal{V}} \frac{\partial_T(su_\perp)}{\partial_T(su_0)}, \tag{32}$$

where $\mathcal{V} \equiv \frac{\partial_T x_\perp(T)}{\partial_T \tau(T)}$ is the average, temperature-dependent, expansion rate. Indeed, this ratio governs the effect of the time-gradient compared with a typical transverse one. Note, however that the *overall* transverse entropy gradient is zero, by virtue of Eq. (4).

In Eq. (32), we have replaced the kinematical variables by their temperature-dependent averages defined by our solution. The approximation range of a transversally isentropic flow is thus related to the value of the (analytically known) expression (32) to be larger than 1 in a significant range of reduced time. In the top graph of Fig. 4 one sees that the transverse over longitudinal entropy gradient becomes indeed significantly larger than 1 for a sufficiently high speed of sound. For a low speed of sound this requires a longer reduced time. This could explain the features of Fig. 3, bottom, with a "retarded" ordering with regard to Ref. [15].

To test the consistency of the quasi-stationary approach (b), in the bottom graph of Fig. 4 we present the expansion rate itself $\mathcal{V} \equiv \frac{\partial_T x_\perp(T)}{\partial_T \tau(T)}$, where the functions $\tau(T)$ and $x_\perp(T)$ are analytically obtained from their definition within our temperature-dependent scheme, namely from Eqs. (2) and (10), respectively. Note that this rate is also appearing in the denominator of Eq. (32), which shows that the two hypotheses of a transversally isentropic flow and a quasi-stationary transverse flow are indeed connected, because a slow motion gives rise to a high transverse over time typical

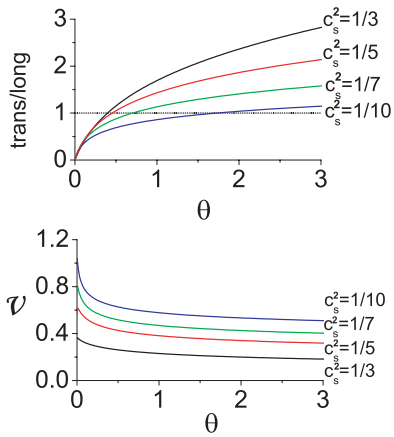

FIG. 4. (Color online) Comparison of entropy and kinematic gradients. The analytically known quantities $\partial_{x_\perp}(su_\perp)/\partial_\tau(su_0)$ and $\mathcal{V} \equiv \partial_T(x_\perp)/\partial_T(\tau)$ (see text) are plotted as a function of the reduced time θ.

entropy gradient. From Fig. 4 we see that both the transversally isentropic and quasi-stationary hypotheses are consistent at not too short reduced times and not too small speed of sound. Thus, these hypotheses give a qualitative analytic understanding of the transverse flow. Our qualitative picture seems consistent. However, the time gradient is not negligible with regard to the transverse derivative, indicating, at least within the initial conditions we chose, that a quantitative agreement could be more difficult to be obtained.

Another topic is the range of validity of our approximation in transverse space. Indeed, because of Eq. (6), the quasi-stationary approach is only valid in the supersonic dilatation regime, which requires a large enough transverse velocity, $v_\perp \geqslant c_s$. This could limit the range of validity of the hydrodynamical flow that has been observed only at small transverse momentum. It could also compromise the dominance of the longitudinal Bjorken flow determining the thermodynamical relations (2). We think that this limitation, which should be taken into account for a quantitative study difficult to perform analytically, will not endanger the qualitative but explicit solution we found. The study of the implications for the transverse momentum dependence of the elliptic flow deserves per se a study that goes beyond the scope of the present work, where no mass relation between fluid velocity and transverse momentum has been introduced.

As an outlook, it will be interesting to develop the study of hydrodynamical mechanisms generating the elliptic flow by the investigation of other phenomenological aspects, such as the above-mentioned $p_\perp$ dependence and the effect of a weak viscosity. To reach more quantitative features, it will be useful to refine the definition of the initial conditions. In fact, it could be worthwhile to typically define *a priori* the dependence of ε as a function of ρ or centrality and find the corresponding initial conditions[3] by inverting, e.g., Eq. (24), in particular, to examine whether they could identify more definitely the hydrodynamical mechanisms. On a more theoretical ground, the existence of rather simple mechanisms may facilitate the search for a relation to the fundamental gauge field theory and in particular the gauge/gravity dual approach of the elliptic flow.

All in all, our results suggest an analytic approach to the transverse motion of the fluid, which can clarify the behavior of the elliptic flow obtained from the data or numerical simulations. This is related to an approximate quasi-stationary property and a transversally isentropic property of the transverse flow for which the time dependence of the system comes mainly through the temperature.

ACKNOWLEDGMENTS

We thank Jean-Yves Ollitrault for his suggestions and remarks and acknowledge fruitful discussions with Guillaume Beuf, Andrzej Bialas, Clément Gombaud, and Wojciech Florkowski. We thank I. M. Khalatnikov and A. Y. Kamenshchik for useful communication. One of us (E.N.S.)

[3]We thank C. Gombeaud for this suggestion.

thanks the IPhT (Saclay) for hospitality during the achievement of this work.

APPENDIX: QUASI-STATIONARY TRANSVERSE FLOW OF A PERFECT FLUID

In this section we derive the basic equations determining the quasi-stationary transverse flow of a perfect fluid. The energy-momentum tensor of a perfect fluid is

$$T^{\mu\nu} = (e+p)u^\mu u^\nu - p\eta^{\mu\nu}, \tag{A1}$$

where e is the energy density, p is the pressure, and u^μ ($\mu = \{0, 1, 2, 3\}$) is the four-velocity in the Minkowski metric $\eta^{\mu\nu}$, with signature $(1, -1, -1, -1)$. It obeys the equations

$$\partial_\mu T^\mu_\nu = 0 \Rightarrow u_\nu \partial_\mu[(e+p)u^\mu] + (e+p)u^\mu \partial_\mu u_\nu - \partial_\nu p = 0, \tag{A2}$$

with $u_\nu u^\nu = 1$, and thus

$$u_\nu \partial_\mu u^\nu = 0. \tag{A3}$$

From now on and for simplicity, ∂_μ denotes ∂_{x_μ}. Multiplying the equations of motion (A2) by u_ν, i.e., projecting them on the direction of the four-velocity, and using Eq. (A3) we acquire

$$\partial_\mu[(e+p)u^\mu] - u^\mu \partial_\mu p = 0. \tag{A4}$$

Finally, reinserting Eq. (A4) into Eq. (A2) we obtain

$$(e+p)u^\mu \partial_\mu u_\nu = -u_\nu u^\mu \partial_\mu p + \partial_\nu p. \tag{A5}$$

Relation (A5) holds for a general perfect fluid. For a stationary flow it gives rise to the Bernoulli equation [11], namely

$$Tu_0 = T_0. \tag{A6}$$

Let us now focus on the stationary transverse flow [7], namely setting $u_3 = 0$, which is the regime of interest of the present work. In this case the equation of motion (A5) for u_3 gives $\partial_3 p = 0$ and thus the various quantities do not depend on the longitudinal coordinate x_3. Therefore, e, p, and the velocities are functions of x_1, x_2 only. The equations of motion (A5) boil down to

$$\begin{aligned} \partial_1\big[(e+p)u_1^2 + p\big] + \partial_2[(e+p)u_1u_2] &= 0 \\ \partial_1[(e+p)u_1u_2] + \partial_2\big[(e+p)u_2^2 + p\big] &= 0 \\ \partial_1[(e+p)u_1u_0] + \partial_2[(e+p)u_2u_0] &= 0, \end{aligned} \tag{A7}$$

with $u_0^2 = 1 + u_1^2 + u_2^2$. Equations (A7) can be expressed in terms of the temperature and the entropy density. Considering vanishing chemical potential we have

$$p + e = Ts; \quad de = Tds; \quad dp = sdT. \tag{A8}$$

Using relations (A8), Eqs. (A7) become

$$\partial_1\big[(Ts)u_1^2\big] + s\partial_1 T + \partial_2[(Ts)u_1u_2] = 0 \tag{A9}$$

$$\partial_1[(Ts)u_1u_2] + \partial_2\big[(Ts)u_2^2\big] + s\partial_2 T = 0 \tag{A10}$$

$$\partial_1[(Ts)u_1u_0] + \partial_2[(Ts)u_2u_0] = 0. \tag{A11}$$

Now, the Bernoulli equation (A6) allows one to transform Eq. (A11) to the entropy conservation in the transverse plane:

$$\partial_1(su_1) + \partial_2(su_2) = 0. \tag{A12}$$

Finally, Eqs. (A9) and (A10), with the use of Eqs. (A3), (A6), and (A11), give rise to the same equation:

$$\partial_1(Tu_2) = \partial_2(Tu_1). \tag{A13}$$

[1] T. Hirano, N. van der Kolk, and A. Bilandzic, arXiv:0808.2684 [nucl-th].
[2] C. Y. Wong, Phys. Lett. **B88**, 39 (1979).
[3] J. Y. Ollitrault, Phys. Rev. D **46**, 229 (1992).
[4] L. D. Landau, Izv. Akad. Nauk Ser. Fiz. **17**, 51 (1953) (in Russian) [English translation: *Collected Papers of L. D. Landau*, edited by D. ter Haar (Gordon and Breach, New York, 1968)].
[5] J. D. Bjorken, Phys. Rev. D **27**, 140 (1983).
[6] A. Bialas, M. Chojnacki, and W. Florkowski, Phys. Lett. **B661**, 325 (2008).
[7] I. M. Khalatnikov and A. Y. Kamenshchik, Phys. Lett. **A331**, 12 (2004).
[8] I. M. Khalatnikov, Zh. Eksp. Teor. Fiz. **26**, 529 (1954) (in Russian). For an English version, see Ref. [9], with a correction of the equation for the potential.
[9] S. Z. Belenkij and L. D. Landau, Nuovo Cimento Suppl. **3**, S10 15 (1956) [Usp. Fiz. Nauk **56**, 309 (1955)]; L. D. Landau and S. Z. Belenkij, in *Collected Papers of L. D. Landau*, edited by D. ter Haar (Gordon and Breach, New York, 1968), Paper No. 88, p. 665 (the derivation of Khalatnikov's solution is not given in Nuovo Cimento's version).
[10] G. Beuf, R. Peschanski, and E. N. Saridakis, Phys. Rev. C **78**, 064909 (2008); G. Beuf, Ph.D. thesis, 2009 (in French).
[11] L. D. Landau and E. M. Lifshitz, *Fluid Mechanics* (Pergamon Press, Oxford, UK, 1987). See also J. Y. Ollitrault, Eur. J. Phys. **29**, 275 (2008), for the hydrodynamics of heavy-ion collisions.
[12] G. A. Milekhin, Zh. Eksp. Teor. Fiz. **35**, 1185 (1958) [Sov. Phys. JETP **35**, 829 (1959)].
[13] I. S. Gradshteyn and I. M. Ryzhik, *Table of Integrals, Series, and Products*, 7th ed., edited by Alan Jeffrey and Daniel Zwillinger (Academic Press, San Diego, 2007).
[14] P. F. Kolb and U. W. Heinz, arXiv:nucl-th/0305084.
[15] R. S. Bhalerao, J. P. Blaizot, N. Borghini, and J. Y. Ollitrault, Phys. Lett. **B627**, 49 (2005).